Journal of Rock Mechanics and Geotechnical Engineering

Journal online: www.rockgeotech.org

A new classification of seepage control mechanisms in geotechnical engineering

Yifeng Chen[1, 2], Ran Hu[1, 2], Chuangbing Zhou[1, 2*], Dianqing Li[1, 2], Guan Rong[1, 2], Qinghui Jiang[1, 2]

[1] *State Key Laboratory of Water Resources and Hydropower Engineering Science, Wuhan University, Wuhan, 430072, China*

[2] *Key Laboratory of Rock Mechanics in Hydraulic Structural Engineering of Ministry of Education, Wuhan University, Wuhan, 430072, China*

Received 14 July 2010; received in revised form 1 September 2010; accepted 6 September 2010

Abstract: Seepage flow through soils, rocks and geotechnical structures has a great influence on their stabilities and performances, and seepage control is a critical technological issue in engineering practices. The physical mechanisms associated with various engineering measures for seepage control are investigated from a new perspective within the framework of continuum mechanics; and an equation-based classification of seepage control mechanisms is proposed according to their roles in the mathematical models for seepage flow, including control mechanisms by coupled processes, initial states, boundary conditions and hydraulic properties. The effects of each mechanism on seepage control are illustrated with examples in hydroelectric engineering and radioactive waste disposal, and hence the reasonability of classification is demonstrated. Advice on performance assessment and optimization design of the seepage control systems in geotechnical engineering is provided, and the suggested procedure would serve as a useful guidance for cost-effective control of seepage flow in various engineering practices.

Key words: seepage flow; seepage control mechanisms; optimization design; coupled processes; initial states; boundary conditions; hydraulic properties

1 Introduction

It has been well recognized in geotechnical engineering practice (dams, slopes, landslides, underground spaces, etc.) that groundwater seepage (flow) has a great influence on the deformation and stability of soils, rocks and geotechnical structures. Seepage control is critical for maintaining the stability and safety of the engineering works [1–16]. Understanding the physical mechanisms and their corresponding numerical modeling approaches of engineering measures for seepage control is obviously of paramount importance for safety assessment, optimization design, construction and operation of a seepage control system.

A large number of engineering measures have been widely taken for seepage control in geotechnical and geoenvironmental engineering practices, and they can generally be classified into four categories. The first category involves in the construction of an impervious zone with low permeability and high critical hydraulic gradient to limit the quantity of seepage flow, reduce the pore water pressure, and preserve the geometrical integrity of the impervious system, such as clay core, asphalt-concrete core, concrete face slab or impervious blanket in embankments, grouting curtain in rock foundations, etc.. The second category employs filter and drain zones in soil/rock foundations, underground caverns and concrete/soil dams to reduce pore water pressure (especially the uplift pressure), collect and remove seepage water, and prevent soils from seepage failure, such as drainage holes, wells, tunnels, prisms or horizontal drainage blankets. The third category is associated with the operation and management of the reservoir, such as the control of the effect of water level fluctuation on groundwater movement. The last one is to improve, by various groundwater remediation techniques, the quality of polluted or contaminated water that may cause hazards to environments and society.

The movement of groundwater in fractured porous media is governed by the mass and the momentum

Doi: 10.3724/SP.J.1235.2010.00209

*Corresponding author. Tel: +86-27-68772221;
E-mail: cbzhou@whu.edu.cn

Supported by the National Natural Science Foundation of China (51079107, 50839004) and the Program for New Century Excellent Talents in University (NCET-09-0610)

conservation laws of water, with the latter commonly being represented by the well-known Darcy's law, and subjected to the constraints of initial conditions, boundary conditions, material properties and computational requirements when numerical modeling is needed. Theoretically, the seepage flow process will be altered or controlled by changing, adding or removing the storage terms in the governing equation, changes of the initial and boundary conditions, or changes of the hydraulic properties as the process evolves [15]. Thus, it is essential to understand the physical mechanisms of various engineering measures for seepage control by linking the control effects with corresponding components in the mathematical model of seepage flow, i.e. governing equation together with initial and boundary conditions and computational parameters. By doing so, performance assessment and optimization design of the seepage control structures can be established on a more rigorous mathematical basis and a sounder scientific foundation.

Based on the knowledge and experiences accumulated in analysis of seepage flow and its control effects in geotechnical engineering [7, 9, 13–15, 17], the physical mechanisms for seepage control are examined in this paper from a new perspective, and an equation-based classification is proposed within the framework of continuum mechanics [18]. The seepage control mechanisms are illustrated with various examples in dam engineering, underground engineering or nuclear waste disposal, and advice is provided on optimization design of a seepage control system.

2 Physical mechanisms for seepage control

2.1 Mathematical model for seepage flow problems

In the most general sense from the viewpoint of continuum mechanics [18], the seepage flow through a deformable unsaturated porous medium undergoing small deformation is governed by the following mass conservation equation [17]:

$$-\nabla(\rho_{\mathrm{w}}\boldsymbol{v}) = \frac{\partial}{\partial t}(\rho_{\mathrm{w}} n S_{\mathrm{r}}) + \rho_{\mathrm{w}} n S_{\mathrm{r}} \frac{\partial \varepsilon_{\mathrm{v}}}{\partial t} + \rho_{\mathrm{w}} j_{\mathrm{lg}} \tag{1}$$

where t is the time, $\boldsymbol{v}$ is the velocity vector of water with respect to the solid skeleton, ε_{v} is the volumetric strain, n is the porosity of the medium, S_{r} is the degree of saturation, ρ_{w} is the density of water, and j_{lg} is the rate of moisture transfer between the liquid and gas phases.

According to the generalized Darcy's law, and considering the thermo-osmosis effect of thermal gradient on water flow, the relative apparent velocity of water [17, 19, 20] can be written as

$$\boldsymbol{v} = -\frac{k_{\mathrm{r}}\boldsymbol{k}}{\mu_{\mathrm{w}}}(\nabla p - \rho_{\mathrm{w}} g) - \boldsymbol{k}_{\mathrm{T}}\nabla T \tag{2}$$

where $\boldsymbol{k}$ is the intrinsic permeability tensor of the medium, k_{r} is the relative permeability of water, $\boldsymbol{k}_{\mathrm{T}}$ is the thermal coupling tensor for water flux, μ_{w} is the dynamic viscosity of water, p is the pore water pressure, T is the temperature, and g is the gravitational acceleration.

The governing equation, Eq.(1), is subjected to the following initial conditions at $t = t_0$:

$$p(x,y,z,t)\big|_{t=t_0} = p_0(x,y,z) \quad \text{(in domain } \Omega\text{)} \tag{3}$$

and the following boundary conditions on Γ:

(1) The Dirichlet (water pressure) boundary condition:

$$p(x,y,z,t) = \overline{p} \qquad (\text{on } \Gamma_p) \tag{4}$$

(2) The Neumann (water flux) boundary condition:

$$q_{\mathrm{n}}(x,y,z,t) \equiv -\rho_{\mathrm{w}}\boldsymbol{v}\boldsymbol{n} = \overline{q} \quad (\text{on } \Gamma_q) \tag{5}$$

where p_0 is the initial pore water pressure, $\overline{p}$ is the prescribed pore water pressure on Γ_p, $\overline{q}$ is the prescribed water flux on Γ_q, and $\boldsymbol{n}$ is the outward unit normal vector to the boundary.

In some engineering practices, only the seepage flow in the saturated domain Ω_{w} is of the main interest. In this case, Eqs.(1) and (2) can be reduced to the following equations, in which the compressibility of the solid skeleton and the thermo-osmosis effect are neglected [13]:

$$[1 - H(\phi - z)]\rho_{\mathrm{w}}\left(\frac{\partial \varepsilon_{\mathrm{v}}}{\partial t} + S_{\mathrm{w}}\frac{\partial \phi}{\partial t}\right) + \nabla(\rho_{\mathrm{w}}\boldsymbol{v}) = 0 \quad \text{(in domain } \Omega\text{)} \tag{6}$$

$$\boldsymbol{v} = -[1 - H(\phi - z)]\boldsymbol{k}\nabla\phi = -\boldsymbol{k}\nabla\phi + \boldsymbol{v}_0 \tag{7}$$

$$\boldsymbol{v}_0 = H(\phi - z)\boldsymbol{k}\nabla\phi \tag{8}$$

where $\boldsymbol{v}_0$ is the initial flow velocity vector introduced to eliminate the virtual flow velocity on the dry domain Ω_{d}, $\phi = z + p/(\rho_{\mathrm{w}} g)$ is the total water head, z is the vertical coordinate, $S_{\mathrm{w}} \equiv \rho_{\mathrm{w}} g n \beta_{\mathrm{w}}$ is the specific storage due to the water compressibility, and β_{w} is the compressibility coefficient of water. The term $H(\phi - z)$ is a Heaviside function to indicate the fact that the unsteady seepage flow through domain Ω is actually the flow through the wet domain Ω_{w}

below the free surface Γ_f, defined as

$$H(\phi - z) = \begin{cases} 0 & (\phi \geq z, \quad \text{in domain } \Omega_w) \\ 1 & (\phi < z, \quad \text{in domain } \Omega_d) \end{cases} \tag{9}$$

Accordingly, the initial and boundary conditions for Eq.(6) are given as

(1) The initial condition:

$$\phi(x, y, z, t)\big|_{t=t_0} = \phi_0(x, y, z) \qquad (\text{in domain } \Omega) \tag{10}$$

where $\phi_0(x, y, z)$ is the initial water head.

(2) The water head boundary condition:

$$\phi(x, y, z, t) = \overline{\phi} \qquad (\text{on } \Gamma_\phi) \tag{11}$$

where $\overline{\phi}$ is the prescribed water head on Γ_ϕ.

(3) The flux boundary condition:

$$q_n(x, y, z, t) \equiv -\rho_w \boldsymbol{v}\boldsymbol{n} = \overline{q} \qquad (\text{on } \Gamma_q) \tag{12}$$

(4) The boundary condition of Signorini's type on the seepage surface [9, 13, 21]:

$$\phi \leq z, \quad q_n \leq 0, \quad (\phi - z) q_n = 0 \qquad (\text{on } \Gamma_s) \tag{13}$$

where Γ_s is the potential seepage boundary.

(5) The boundary condition of flux on free surface:

$$q_n \equiv q_n|_{\Omega_w} - q_n|_{\Omega_d} = -\boldsymbol{n}\left(\rho_w \mu \frac{\partial \phi}{\partial t} \boldsymbol{e}_z\right) \qquad (\text{on } \Gamma_f) \tag{14}$$

where $\Gamma_f \equiv \{(x, y, z)|_{\phi=z}\}$ is the free surface, an interface between Ω_w and Ω_d; μ is the gravitational specific yield; $\boldsymbol{e}_z = \{0, 0, 1\}^T$ is the upward vertical unit vector.

Equation (14) obviously describes the release or storage of water in the media due to fluctuation of water table, and it is an inner boundary condition as the problem is formulated on the entire domain. This condition actually indicates the Rankine-Hugoniot jump condition of flux on the propagation front of the non-steady seepage flow across which discontinuities are involved in the normal direction [22].

It is to be noted that if the dependence of ϕ on t vanishes, the governing equation, Eq.(6), along with the boundary conditions, Eqs.(11)–(14) for unsteady seepage flow, immediately reduces to its steady state counterpart.

2.2 Equation-based analysis of seepage control mechanisms

From Section 2.1, it can be inferred that the movement of groundwater flow is governed by the continuity equation, together with the initial and boundary conditions and a set of hydraulic properties of the media. Solving the equation yields the evolutions and distributions of the basic unknowns (water head, pore water pressure and free surface) and the derivative unknowns (hydraulic gradient, flow velocity, flow rate through a particular cross-section, seepage boundary, etc.) of a seepage field. It is the seepage control that produces a seepage field favorable to engineering stability and safety, and the control measures may take effects by changing the storage terms in the governing equations, the initial and boundary conditions, and the hydraulic properties of the media [15]. Therefore, the physical mechanisms associated with various engineering measures for seepage control can correspondingly be classified into the following four types: control by processes, control by initial states, control by boundary conditions and control by hydraulic properties.

The first mechanism (i.e. control by processes) is associated with the coupling effects between water flow, thermal transport, stress/deformation and even chemo-biological processes in the media. Although a complete model for the coupled thermo-hydro-mechanical (THM) phenomena in geological porous media [17] is not presented in this context, Eqs.(1) and (2) clearly show the coupling effects of deformation, heat transport and gas transport on movement of groundwater. The deformation of the media not only leads to changes in the storages terms in Eq.(1) through the porosity n and the volumetric strain ε_v, but also results in change in flow velocity in Eq.(2) through the intrinsic permeability tensor $\boldsymbol{k}$. The heat transport may induce water flow through the thermo-osmosis effect presented in Eq.(2), and trigger the changes in mechanical behavior and hence the hydraulic behavior of the media through thermal expansion and thermal damage. Furthermore, the moisture transfer rate j_{lg} in Eq.(1) is also closely related to the temperature T. Finally, the degree of saturation S_r is related to both water and gas transports in unsaturated zone of the domain, even though the gas flow behavior is difficult to be controlled in practice.

Therefore, it is possible to control the seepage flow process by stimulating or restraining other transport processes in the coupled system, provided that the coupling effects between the processes are strong and the corresponding engineering measures are cost-effective. Applying the control mechanism may result in expansion or contraction of the storage terms of the governing equation, or lead to changes in hydraulic properties of the media in a well-controlled manner. This mechanism may be particularly attractive in controlling water flow and radionuclide migration in an underground radioactive waste disposal system or in groundwater remediation for removing pollutants and contaminants from the groundwater.

The second mechanism (i.e. control by initial states) is available due to the fact that the initial distribution

of pore water pressure (or head), as shown in Eq.(3) or (10), has a dominant influence on the water movement in the near term. The initial state of the seepage field can be changed by pumping or draining groundwater before a project starts, and as a result, the seepage flow will be controlled in a near period of time, which may be applicable during construction or reinforcement of some engineering works.

The third mechanism (i.e. control by boundary conditions) takes the advantage of the strong constraints of boundary conditions on seepage flow and has been commonly applied to groundwater flow control in dams, slopes, mining, etc.. The deployment of drainage holes, tunnels and prisms in such engineering practices changes the boundary conditions of the seepage problem through Eq.(5) or (13) by presenting new flow or seepage boundaries, hence changing the distribution of pore water pressure, keeping the working area of a project in dry or dryer state, and eliminating the possible negative effects of seepage flow. Furthermore, a proper operation scheme of reservoir maintains a low fluctuation rate of reservoir water level, and avoids the abrupt change in water head boundary conditions (cf. Eq.(3) or (10)) in a reservoir area. As a result, the seepage flow induced landslides may also be effectively reduced.

The last mechanism (i.e. control by hydraulic properties) aims to control the seepage flow through changes in the internal hydraulic properties of the materials, such as permeability $\boldsymbol{k}$ in Eq.(2) or (7), specific yield μ in Eq.(14), critical hydraulic gradient J_{cr} (a material parameter used for judging if seepage failure occurs), water retention curves (the dependence of degree of saturation and relative permeability on water pressure, i.e. S_r–p and k_r–p relations, in unsaturated condition). The impervious and filter zones widely employed in dam engineering take effect by this mechanism. In addition, as stated before, the seepage control mechanism by coupled processes functions at least partly through the changes in hydraulic properties. In this sense, it is one of the most important mechanisms for seepage control.

The above classification of seepage control mechanisms has clear physical significance and each engineering measure can be rigorously represented in the mathematical model of seepage flow. It should be noted, however, that different mechanisms have different sensitivities and effectivenesses for seepage control. The control mechanisms by boundary conditions and hydraulic properties are obviously the most sensitive and effective ones, and they have been successfully and widely applied to engineering practices. The mechanism by coupled processes is also effective provided that the coupled processes would result in remarkable changes in hydraulic properties and storage terms, and it is justified by the increasing interests in the coupled THM analysis of fractured porous media. Finally, the control mechanism by initial states is only valid in the near term, and the lower the permeability and the initial water content of the media are, the longer the effects of control period of time may last. This is exactly the reason that the control of initial water content of low-permeability bentonite blocks during manufacture is so important for the wetting process of the engineered barriers in the nuclear waste repositories [23].

3 Illustration of seepage control effects

3.1 Seepage control by coupled processes

To illustrate the seepage control mechanism by coupled processes, here we focus on the moisture transfer in an engineered barrier system of nuclear waste repository. As proved by both in-situ experiments and theoretical predications [24, 25], the excavation of tunnels in a hard rock may induce an increase in permeability up to 3 orders of magnitude in the disturbed zone. Then, as compacted expansive clay blocks are placed in the surrounding space of the host rock, deformations of the barrier materials resulted from thermal expansion and moisture swelling are constrained, hence impact the water flow by changes in storage terms (porosity, volumetric strain, and density) and hydraulic properties (permeability and water retention curves). In addition, the heat generated by the radioactive decay of the waste may have an impact on the water flow by the thermo-osmosis effect of the clay materials in the engineered barriers. By choosing clay materials with different swelling and thermal coupling properties, altering these properties in the manufacturing process, or restraining the significant excavation-induced increase in permeability in the surrounding rocks with some well-controlled tunneling techniques, the water flow process may be controlled to some extent.

To show the possible control of water flow by heat transport, we take the CEA Mock-up test [26] for the THM behaviors of the compacted MX-80 bentonite buffer for nuclear waste disposal subjected to high

temperature (up to 150 °C) and large thermal gradient (up to 640 °C/m on average) for example. Interested readers may refer to details of the experimental setup and test procedure in Ref.[26]. In Refs.[17, 27], a fully coupled THM analysis of the test was performed with the finite element code THYME^{3D}, with the physical mechanisms of the coupled processes that are well demonstrated.

According to the modeling results, it has been found that the thermo-osmosis effect takes negligible effect on the moisture transfer in the bentonite sample, and the evolutions of relative humidity measured by 7 capacitive sensors installed at different heights of the sample can be best fitted by assuming isotropic thermal coupling with a thermal coupling coefficient $\boldsymbol{k}_T = 0$ m^2/(s·K) in Eq.(2). The corresponding evolutions of the degree of saturation S_r at various heights of the sample are plotted in Fig.1(a). However, if the thermal coupling coefficient is assumed to vary linearly with the degree of saturation, i.e. $\boldsymbol{k}_T = k_{T0}S_r$, by applying some control mechanisms in the manufacturing procedure of the sample, with the value in saturated state $k_{T0} = 2\times10^{-12}$ m^2/(s·K) (a value comparable to that adopted for the FEBEX bentonite [17]), the degree of saturation will evolve in the manner shown in Fig.1(b). Comparison of Figs.1(a), (b) shows very different distribution and evolution patterns of water content in the sample, only due to the thermo-osmosis effect by moving water in the negative direction of thermal gradient. Obviously, the stronger the thermo-osmosis effect is, the longer the period of time will be needed for full re-saturation of the sample, which is an important measure for designing a nuclear waste repository.

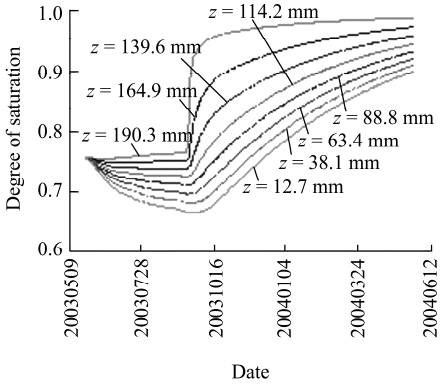

(a) Negligible thermo-osmosis effect ($k_{T0} = 0$ m^2/(s·K)).

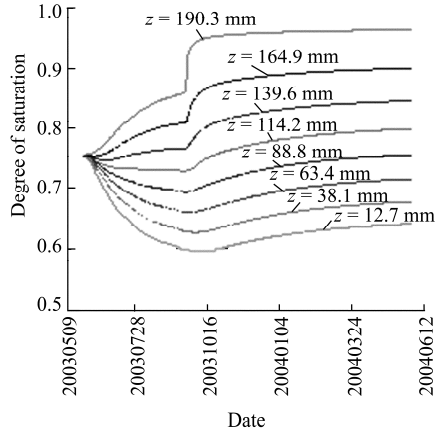

(b) Moderate thermo-osmosis effect ($k_{T0} = 2\times10^{-12}$ m^2/(s·K)).

Fig.1 Evolutions of the degree of saturation in the bentonite sample with different thermal coupling effects.

3.2 Seepage control by initial states

As stated before, the initial distribution of water content (or equivalently, suction in soil mechanics) will lead to very different wetting processes in a low-permeability engineered barrier. In dam engineering, the initial distribution of pore water head in the strata of the dam site also plays an important role in the near-term evolution of seepage field, indicating the significance for site investigation and characterization about hydrological conditions and the possibility in controlling the seepage flow by changing its initial condition.

As an example, we consider the seepage flow process in the concrete faced rockfill dam (CFRD) in the Shuibuya hydropower project. The CFRD is 233 m high, which is up to now the highest of its kind of dams in the world. Interested readers may refer to Refs.[13, 16, 28] for the profile, the material zoning and the construction schedule of the CFRD, the monitoring instrumentations and the geological and hydrological conditions in the dam site.

The seepage flow in the CFRD is characterized with the unsteady seepage flow model presented in Section 2.1, and solved with a newly-developed parabolic variational inequality (PVI) formulation of Signorini's condition [13]. The construction process of the CFRD started on March 1, 2003 and lasted for 52.5 months. The impounding process of the reservoir started on October 19, 2006. Therefore, the numerical modeling of the seepage flow process started on March 1, 2003 and ended on May 11, 2008. The initial distribution of water head was determined with a steady state seepage analysis by taking into account the hydrological conditions in the dam site before construction.

Without going into details of the finite element model and the computational parameters of the dam materials and strata, which can be referred to Ref.[28], we plot in Fig.2 the evolutions of measured and computed pore water pressure heads at two typical

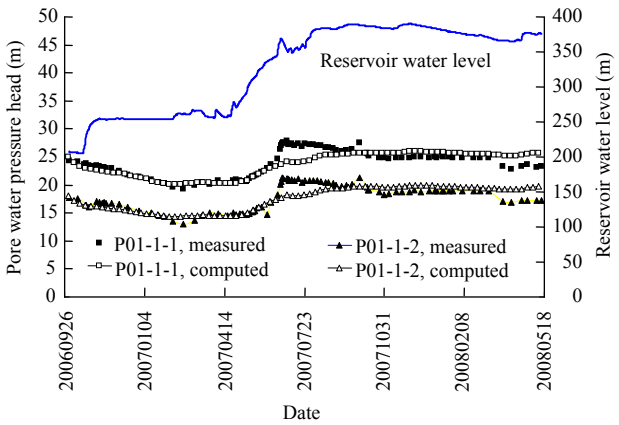

Fig.2 Comparisons of measured and calculated pore water pressure heads at two typical piezometers in Shuibuya CFRD.

piezometers installed at the maximum cross-section of the CFRD, numbered by P01-1-1 and P01-1-2, respectively. Also the variation of the reservoir water level is shown in Fig.2. It can be observed from Fig.2 that the computed water pressure heads generally have a rather good agreement with the measurements.

It is interesting to see from Fig.2 that during initial phase of impounding, the reservoir water level rose from 205.8 m on October 19, 2006 to 254.8 m on November 8, 2006, and it almost maintained constant until February 8, 2007 before a fluctuation started again. Both the measured and computed pore water pressures at the piezometers, however, decreased until February 21, 2007. The underlying mechanism is exactly related to the initial condition of the seepage field. The piezometers, P01-1-1 and P01-1-2, were installed so early on April 18, 2003 and March 19, 2003, respectively, that a hydraulic connection existed between the rock foundation and the filled rockfills before construction of the impervious system composed of face slabs and grouting curtain. After the impervious system became operative, the drainage process in the CFRD lasted for four months even though the reservoir water level was significantly raised.

3.3 Seepage control by boundary conditions

As stated before, the seepage control mechanism by boundary conditions is one of the most effective control mechanisms in engineering practices. Without loss of generality, here we consider the possible boundary conditions of the drainage holes in unsteady seepage flow condition [9], as illustrated in Fig.3. The first type is the water head boundary condition, as depicted in Fig.3(a). The drainage holes deployed in a rock foundation generally possess this type of boundary condition. The prescribed water head is usually

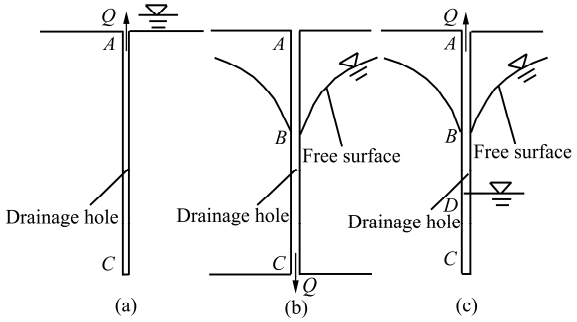

Fig.3 Boundary conditions of drainage holes.

determined by the floor elevation of the drainage tunnel connected with the holes. The second type of boundary condition is the Signorini's type, such as the vertical drainage holes deployed between two horizontal drainage tunnels in a concrete dam, where the drainage flow is always discharged into the lower drainage tunnel. As shown in Fig.3(b), on section *AB* of the drainage hole, the boundary condition satisfies $\phi < z$ and $q_n = 0$, while on section *BC*, it satisfies $\phi = z$ and $q_n \leq 0$.

Associated with a drainage hole in deficiency, the third type of boundary condition is actually a condition with known drainage flow rate of the hole. As shown in Fig.3(c), part of the boundary, i.e. section *AD*, satisfies the complementary condition of Signorini's type, while the other section *DC* satisfies the water head boundary condition (the first type as defined above). The water head in the drainage hole is generally unknown a priori, and has to be determined by its flow rate, *Q*, through an iterative procedure.

The effects of a drainage system composed of drainage holes and tunnels on the seepage flow in a gravity dam can be referred to Ref.[9], in which the depression of free surface, the reduction of uplift pressure, the sensitivity of the deployment pattern of the drainage holes (i.e. spacing and diameter) on the seepage behavior are systematically analyzed.

To further illustrate the control effects of drainage holes and tunnels on groundwater flow, we show the seepage flow process in the surrounding rocks of the Shuibuya underground powerhouse during impounding and operation of the reservoir [13, 14]. The size of the cavern is 168.50 m in length, 23.00 m in width and 65.47 m in height. The strata contain Qixia formation (P_{1q}^{14} - P_{1q}^{1}), Ma'an formation (P_{1ma}), Huanglong formation (C_{2h}) and Xiejingshi formation (D_{3x}), with well developed weak shear zones in the surrounding rocks.

Resulting from the complex geological conditions, the seepage flow control in the surrounding rocks was one of the key technological issues on the safety of the cavern. The seepage control system consisted of a grouting curtain, drainage holes and drainage tunnels, where the drainage tunnels were deployed in three layers at different elevations. The drainage holes were deployed along the axes of the drainage tunnels and connected by the drainage tunnels to form a drainage system. The drainage holes included two categories: vertical holes and inclined holes with an inclination angle of 45°, which were installed alternately with 1.5 m in spacing. In total, 1 557 drainage holes were deployed, with a uniform size of 108 mm in diameter and 30 m in length.

Similarly, the seepage flow was modeled with the unsteady seepage model. The time for numerical modeling started at 8:00 on October 1, 2006 and ended at 8:00 on May 11, 2008. All the surfaces of the drainage tunnels and drainage holes were specified with the potential seepage boundaries satisfying the Signorini's complementary condition, i.e. Eq.(13). More details of the finite element model, computational parameters, and initial and boundary conditions of the cavern can be referred to Ref.[13].

Figure 4 depicts the propagation fronts of the seepage flow at various times. The predictions have been validated by the field measurements of piezometers installed in the surrounding rocks of the cavern and the grouting tunnels below the toe slab of the CFRD [13]. On May 11, 2008, the impounding process of the reservoir was completed (see Fig.2), whereas the free surface at that time was far from reaching the steady state due to significant time lag of the groundwater flow. It can be inferred from Fig.4 that the drainage system formed by the drainage holes and drainage tunnels has a great impact on the evolution of the free surface. Drastic depression of the free surface occurs across the drainage system, and a clear cone of depression is formed in the surrounding rocks of the powerhouse, indicating that the drainage system is reasonably designed, and the seepage flow is effectively controlled. One may observe from Fig.4 that during impounding and operation of the reservoir, the fluctuation of the pool level has little impact on the water table in the surrounding rocks of the cavern, which is obviously favorable for the cavern stability.

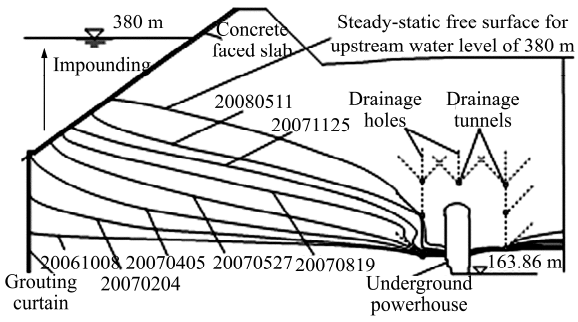

Fig.4 Evolutions of free surface of non-steady seepage flow at various times in the surrounding rocks of the Shuibuya underground powerhouse.

It can be further inferred from Fig.4 that during operation of the project, the drainage holes and drainage tunnels over the depression cone of the water table lose their roles in controlling the seepage flow from the reservoir, but still function for draining the groundwater flow resulted from rainfall infiltration and the possible local aquifers in the surrounding rocks [14]. Since the latter part of water flow is generally typical small flow rate, the number of drainage holes could be moderately reduced, indicating the significance of realistic modeling of the drainage system for optimization design.

3.4 Seepage control by hydraulic properties

The seepage control mechanism by hydraulic properties is another one that has been effectively and widely used in engineering practices. The grouting curtain in rock foundations is first examined here for illustration of the seepage control effects. According to the "Design specification for concrete gravity dams" (SL 319-2005) and the "Design specification for concrete arch dams" (DL/T 5346-2006) in China, the permeability of a grouting curtain in dam foundations must satisfy the following criteria: q = 1–3 Lu for dam height over 100 m; q = 3–5 Lu for dam height between 50 and 100 m; and q = 5 Lu for dam height below 50 m, where q (in Lu or L/(min·MPa·m)) is defined as the flow rate of water per unit water pressure injected into a unit section of borehole at the third (or maximum) pressure step of packer testing after steady-state condition is achieved. As a result, the permeability of the grouted zone is well controlled and an impervious system of integrity is created, hence the undesirable effects of concentrated channel flow through conductive faults, weak zones, joints or fractures could be eliminated.

Another interesting point associated with the control mechanism by hydraulic properties is the excavation or mechanical loading-induced evolution of permeability in rocks, which is the task of control by coupled processes, but it functions partly through variation of permeability. For an individual joint in a hard rock

subjected to normal and shear loads, the post-peak shear dilatancy may lead to an increase in mechanical aperture in one order of magnitude and hence an increase in hydraulic conductivity in 2 orders of magnitude [25, 29]; and for deep-buried intact rocks with sparsely-developed fractures, the excavation-induced increase in hydraulic conductivity in the disturbed zone may approach up to 3 orders of magnitude [24, 29, 30].

This phenomenon was observed in the surrounding rock of the excavated circular tunnel subjected to biaxial stress field in the Stripa mine, Sweden [24]. The radius of the tunnel is about 2.5 m with two major sets of fractures striking obliquely to the tunnel axis. Fracture frequencies measured in holes drilled from the tunnel were on average 4.5 fractures per meter in inclined holes and 2.9 fractures per meter in vertical holes. The initial stress field is anisotropic with a higher horizontal stress component (i.e. 20 MPa in horizontal and 10 MPa in vertical) and the conductivity of the undisturbed host rock, k_0, is about 10^{-10} m/s. The excavation of the test drift produced a dramatic increase in axial hydraulic conductivity in a narrow zone adjacent to the periphery of the drift. The conductivity increase was estimated to be 3 orders of magnitude through a buffer mass test.

The excavation-induced changes in hydraulic conductivities around the circular tunnel were modeled with the theory presented in Ref.[25], as replotted in Fig.5, where the mobilized dilatancy behavior of the fractures in the post-peak loading section was considered. One observes that generally the conductivities in tangential directions increase greatly due to formation of the excavation disturbed zone (EDZ) around the tunnel, while the conductivities in radial directions diminish greatly as a result of closure on related fractures. The maximum increase in hydraulic conductivity matches well with the field observations. It can be inferred from Fig.5 that if the controlled blasting methods were used or the converged displacements were controlled through just-in-time support, the excavation-induced evolution of permeability would be controlled at least to a certain degree.

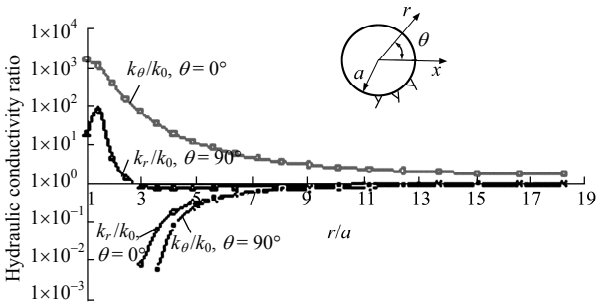

Fig.5 Excavation-induced evolution of hydraulic conductivity around the circular tunnel, where a is the radius of the tunnel and r is the distance away from the tunnel center.

4 Optimization design of seepage control systems

4.1 Procedure for optimization design

With the above equation-based classification of seepage control mechanisms and the control effects of various engineering measures, advice on optimization design of a seepage control system in geotechnical engineering is provided in this section. The suggested flowchart is plotted in Fig.6, which at least has been partly followed in engineering practices (see Refs. [3–6, 16]). The procedure is described as follows:

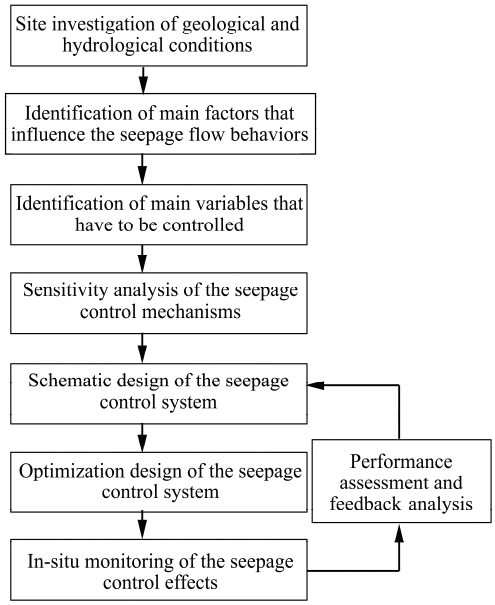

Fig.6 Flowchart of optimization design of a seepage control system.

(1) Site investigation of geological and hydrological conditions

As the first step of optimization design of a seepage control system, comprehensive investigation of geological and hydrogeological conditions in the engineering site is critical for a clear understanding of the initial state of the seepage field, the conducting capability of the media, the resistance of the materials to seepage failure and the in-situ stress field and geothermal conditions of the project. At this step, the degree of fracture development, the potential concentrated flow channels and the correlation

between the permeability and the in-situ stress should be particularly identified.

(2) Identification of main factors that influence the seepage flow behaviors

The main factors that may have an influence on the seepage flow behaviors should be identified according to the hydrological nature of the site. These factors may include, but are not limited to, the initial distribution of water content or pore water pressure in the field, the coupling effects of thermo-mechanical processes on the seepage flow, the hydraulic properties of the media, the boundary conditions of the problem, the climate condition in the area, the preferable engineering measures for seepage control, the possible defects in the seepage control system, etc.. Sensitivities of the factors to the seepage flow should also be preliminarily assessed based on the existing knowledge and experiences that have been accumulated.

(3) Identification of main variables for seepage control

Based on the geological conditions of the site, the properties of materials that will be used and the characteristics of the project, the main variables of seepage control and the corresponding criteria should be indentified. The variables may include, but are not limited to, the seepage flow rate through some particular sections, the distribution of pore water pressure or uplift pressure, the location of free surface, the potential seepage zone, the maximum hydraulic gradient in each medium, the prevention of an impervious zone from seepage failure, the duration of time for re-saturation of an unsaturated medium, the quality of water or the content of contaminants, etc..

Obviously, different engineering practices have different objectives of seepage control. For example, for a gravity concrete dam, the primary control variables may be the seepage flow rates through the dam body, the rock foundation and the abutments of both sides; the distribution of pore water pressure in the dam; and the distribution of uplift pressure at its base. For a nuclear waste repository, the primary control variables may include the re-saturation time of the engineered barriers, the flow velocity in the buffer materials, the possible channeling velocity of flow through conductive discontinuities (e.g. faults, shear zones, dikes or factures) in the host rocks, and the time and the quantities of radionuclides that may reach the biosphere.

(4) Sensitivity analysis of the seepage control mechanisms

The above findings lead to choices of mathematical models most suitable for describing the seepage flow behaviors in the domains of interest. The possible models may include the saturated/unsaturated model, the non-steady state model, the steady state model, or even the discrete fracture network flow model that is out of the scope of this paper. Then the suitability, applicability, reliability and sensitivity of the above-mentioned four mechanisms for seepage control in the project should be analyzed based on the mathematical models selected, together with the initial and boundary conditions of the problem as well as the physical properties of the materials. At this step, theoretical conceptualization and analysis need to be performed, but a predictive numerical analysis is a more powerful tool, even though complicated calculations are involved.

(5) Schematic design of the seepage control system

Designing the seepage control layouts should then be performed according to the mechanisms that may produce the most effective control of the seepage flow and the corresponding measures that are available in engineering practices. A number of design schemes should be proposed, with different combinations of available measures and different layout parameters. For example, the layout parameters for a drainage hole array may include the rows, spacing, lengths and diameters of the hole. For a clay core in soil dams, the layout parameters may be the size of the core, the clay materials that are available in the local site, the granular composition, the compacted density and the optimum water content for compaction.

(6) Optimization design of the seepage control system

The seepage control effects of various design schemes should be appropriately assessed by numerical modeling. The cost and the technical availability of each scheme should also be estimated. The primary control variables, such as the flow rate and the maximum hydraulic gradient, should be particularly checked to find out if they have met the specified criteria. By comparison of the seepage control effects, and the cost and the technical availability between the design schemes, the optimization design of the seepage control system would finally be obtained.

(7) In-situ monitoring of the seepage control effects

After construction of the seepage control system, in-situ monitoring of the seepage control effects should be conducted. The monitoring items may include the evolutions of flow rate, pore water pressure, relative humidity, precipitation, the quality

of water, besides other variables affecting the mechanical stability and functionality of the system. The instrumented sections, zones or points must cover the domain particularly concerned, especially in or around the seepage control system. The monitoring data should be continuously recorded for later use, and as the conditions for seepage flow change, the monitoring interval should be adjusted.

(8) Performance assessment and feedback analysis of the seepage control system

Using the monitoring data, the performance of the seepage control system should then be assessed with a properly designed scheme. If the effects of seepage control do not meet the specified criteria, or significant errors are presented between the numerical predictions in the optimization design stage and the field measurements in the in-situ monitoring stage, feedback analysis of the seepage control effects should be performed to find out the underlying reasons for these errors. Then the design should be adjusted, and the performance should be re-assessed until it meets the design criteria.

4.2 Effects of horizontal drains on slope stability

When the above procedure is applied to a soil slope, the primary objective is to stabilize the slope against the rainfall-induced slope failure. Deployment of horizontal drains has been proven to be one of the most cost-effective engineering measures in improving the slope stability. In Refs.[31, 32], the effects of horizontal drains on the stability of a natural slope and a perfect slope, respectively, were systematically analyzed. In this context, we further investigate the effects of horizontal drains on the stability of an idealized slope during rainfall by mainly taking the drains spacing as the optimization parameter.

4.2.1 *Computational model*

An idealized soil slope with a height of 35 m and a gradient of 1:1 is considered, as shown in Fig.7.

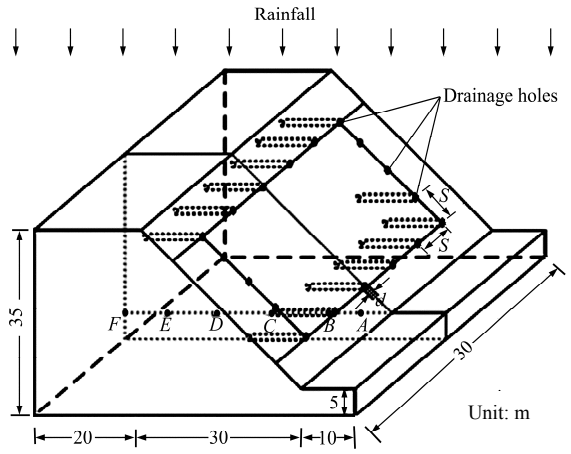

Fig.7 Illustration of an idealized slope under rainfall.

The initial groundwater level is assumed to be horizontal and at the lower ground surface. The initial degree of saturation is assumed to be uniform at the slope crest, with S_r = 0.682, and linearly increases to unity at the height of the initial water level. The van Genuchtan model [33] is adopted to describe the hydraulic characteristics of the soil:

$$S_r = \frac{\theta - \theta_r}{\theta_s - \theta_r} = (1 + |\alpha h|^n)^{-m} \tag{15}$$

$$k(\theta) = k_s k_r = k_s S_r^{\frac{1}{2}} [1 - (1 - S_r^{\frac{1}{m}})^m]^2 \tag{16}$$

where θ is the volumetric water content; θ_s and θ_r are the saturated and residual volumetric water contents, respectively; k_s and k_r are the saturated and the relative hydraulic conductivities, respectively; α, m and n are empirical model parameters, $m = 1 - 1/n$, $n > 1$; and h is the pore water pressure head. The following parameters are taken for analysis: α = 1.0 m^{-1}, n = 1.5, θ_s = 0.469, θ_r = 0.139 and k_s = 6.4×10^{-4} cm/s.

The rainfall of a constant intensity 30 mm/h is assumed to last for 4 day (96 hours). The shear strength of the unsaturated soil during rainfall is represented by the following model:

$$\tau_f = c' + [(\sigma_n - p_a) + \chi(p_a - p_w)] \tan \varphi' \tag{17}$$

where τ_f is the shear strength at failure, σ_n is the total normal stress, p_a is the pore air pressure, p_w is the pore water pressure, c' is the effective cohesion, φ' is the effective friction angle, and χ is the Bishop coefficient. $\sigma_n - p_a$ denotes the net normal stress, and $p_a - p_w$ denotes the matrix suction. The following parameters are taken for analysis: c' = 43 kPa, φ' = 32°, $\chi = S_r$ [34], and γ_s = 19 kN/m^3, where γ_s is the unit weight of soil in natural state.

To improve the slope stability during rainfall, horizontal drains with uniform horizontal and vertical spacings are deployed in the slope, with diameter d = 120 mm, length L = 15 m, and spacing S = 5, 10 and 20 m, respectively, for assessment. For S = 5 m, there are 5 rows of drains in the slope; and for S = 10 and 20 m, there are 3 and 2 rows of drains, respectively, with the top and the lowest rows of drains at the same locations. The boundaries of the drains are specified as unsaturated-saturated potential seepage boundaries. The stability of the slope is assessed with the Morgenstern-Price method [35], together with an automatic search procedure for the critical slip surface. The pore water pressure p_w in Eq.(17) is obtained from the three-dimensional finite element analysis of

transient water flow through the unsaturated-saturated soil, and the total normal stress σ_n on a potential slip surface is estimated by N/l, where N is the normal force acting on the base of a soil slice, and l is the length of the base.

4.2.2 *Effects of horizontal drains*

The evolutions of pressure head without the horizontal drains and those with the drains of spacing S = 5 m during rainfall at 6 observation points in the slope (see Fig.7) are plotted in Fig.8. The observation points are located at the lower ground level and the cross-section along the horizontal drains, and the distances from the points *A*–*F* to the toe of the slope are 5, 10, 20, 30, 40 and 50 m, respectively. The curves clearly show that the groundwater level during rainfall is effectively lowered by the horizontal drains. After 69.0 and 71.5 hours of rainfall for the cases without and with the drains, respectively, there exhibits a sudden rise of groundwater level at the observation points, due to the connection of the perched water with the main groundwater level. At the end of modeling, the discrepancies of pressure head between the above two cases at points *A*–*F* approach 0.80, 2.00, 3.22, 2.90, 2.50 and 2.35 m, respectively.

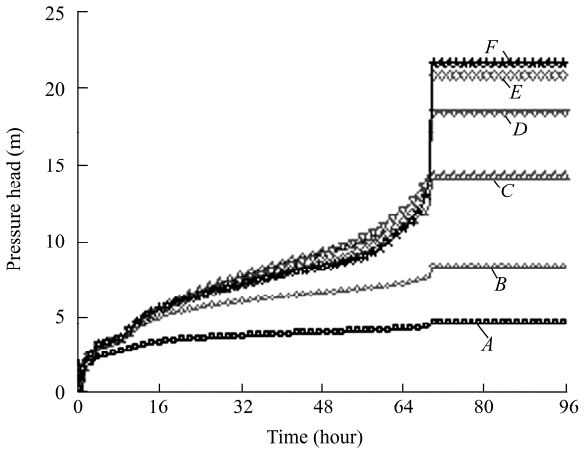

(a) No drains.

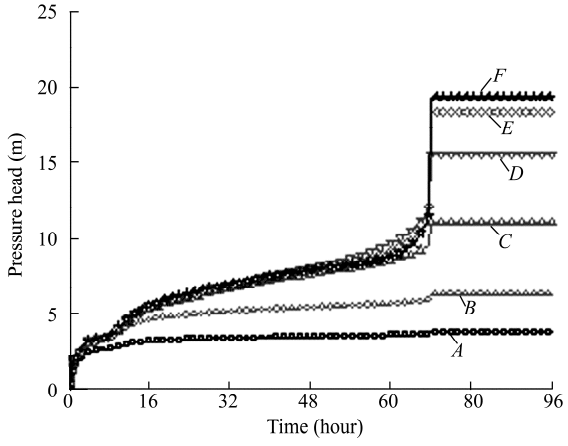

(b) Drains with spacing S = 5 m.

Fig.8 Evolutions of pressure heads with/without drains.

Figures 9–11 plot the distributions of pressure head at the cross-section along the horizontal drains without the drains and with the drains of spacing S = 5 m after rainfall of 24, 48 and 75 hours, respectively. Again, Figs.9–11 clearly show the remarkable effects of the drains on lowering the pore water pressures in the slope. One observes from the figures that there is an unsaturated zone with negative pressure head in the middle of the slope, in other words, there is a perched water zone with positive pressure head above the unsaturated zone. The unsaturated zone becomes smaller as the infiltration of rainfall proceeds, and disappears as the connection occurs suddenly between these two zones and a steady-state flow behavior is then approached.

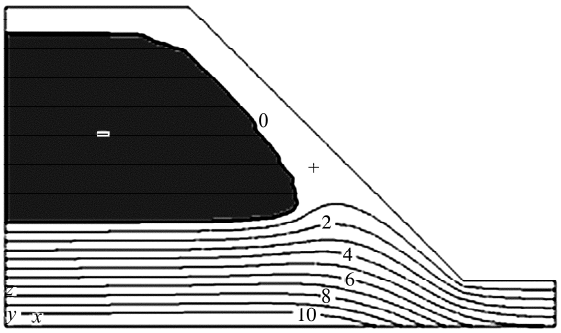

(a) No drains.

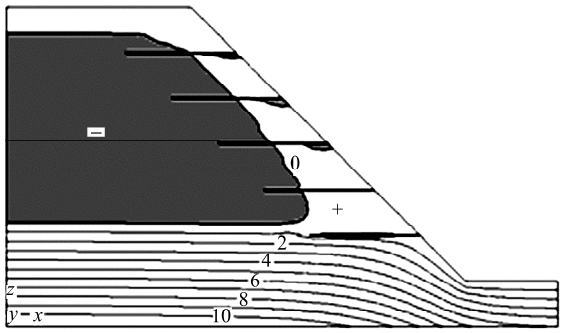

(b) Drains with spacing S = 5 m.

Fig.9 Contours of pressure head after 24 hours of rainfall with/ without drains (unit: m).

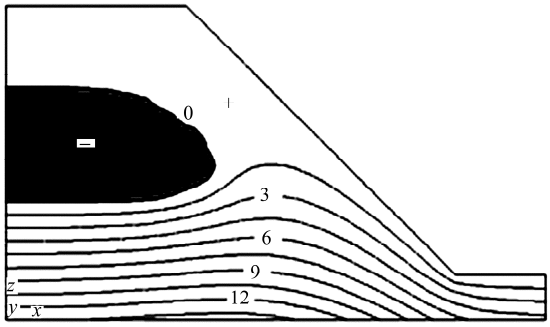

(a) No drains.

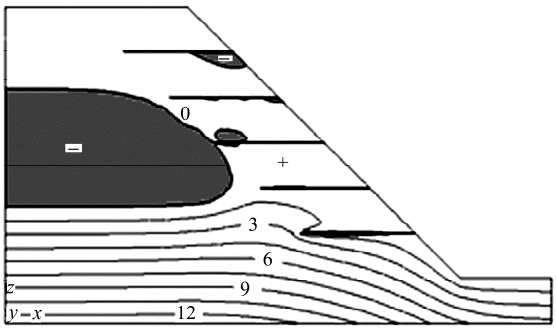

(b) Drains with spacing S = 5 m.

Fig.10 Contours of pressure head after 48 hours of rainfall with/without drains (unit: m).

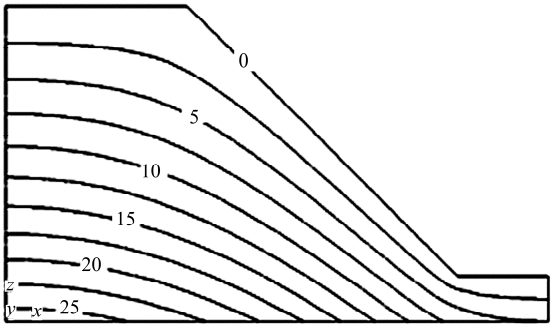

(a) No drains.

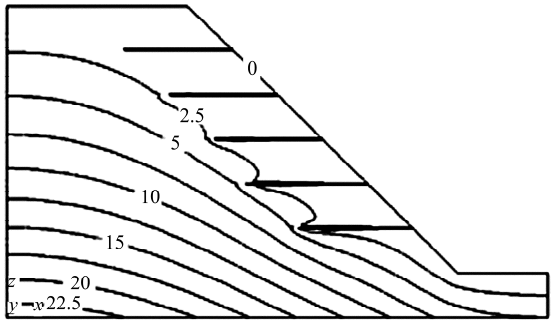

(b) Drains with spacing S = 5 m.

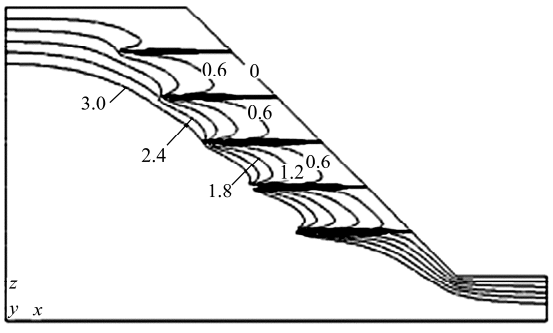

(c) Local distribution of pressure head around the drains.

Fig.11 Contours of pressure head after 75 hours of rainfall with/without drains (unit: m).

Figure 12 shows the evolutions of factor of safety of slope for various deployment schemes of the horizontal drains. The factor of safety at the initial state is 1.40, and it evolves to 1.0 after 69.3 hours of rainfall if no drains are considered, meaning that failure of the slope may theoretically occur at that time and the slope reaches its critical state. As the whole slope is saturated, the factors of safety are 0.95 and 1.08, respectively, for the cases without the horizontal drains and with the drains of S = 5 m. It can be inferred from the curves that denser spacing of the drains would lead to higher stability of the slope, and as the steady state of infiltration is approached, the factors of safety are increased by 0.13, 0.10 and 0.07 for the cases with the drains of S = 5, 10 and 20 m, respectively, compared to the case without the drains. In addition, for the drains with S = 5 m, the top row has a negligible effect on improving the stability of the slope, but the lowest row has a remarkable effect, indicating the importance of the installed locations of the drains in draining out the water and maintaining the stability of the slope.

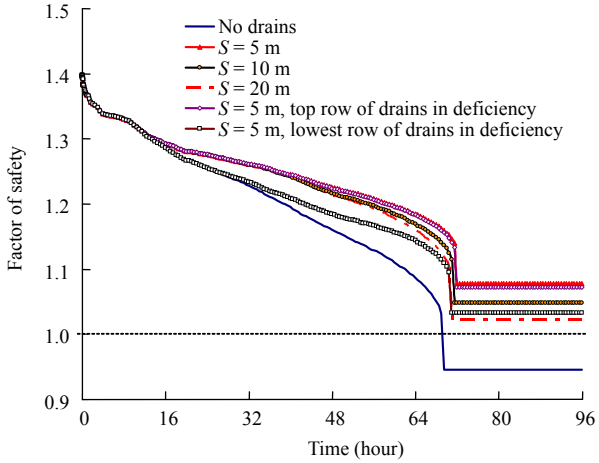

Fig.12 Evolutions of factor of safety for various deployment schemes with/without horizontal drains.

The above calculations show that for this particular slope with extremely large intensity and relatively long duration of rainfall, it is preferable to maintain the slope stability against the rainfall-induced failure by using comprehensive engineering measures, such as drainage, shotcrete support, and cable/bolt support.

5 Conclusions

In this paper, physical mechanisms associated with various measures for seepage control in geotechnical engineering are examined from a new perspective, and are classified, according to their roles in the mathematical models of seepage flow, into four types:

control by coupled processes, control by initial states, control by boundary conditions and control by hydraulic properties. This classification has clear physical and engineering significances and each measure has its mathematical counterparts in the governing equations and computational models. This classification system is obviously of applicability for performance assessment and optimization design of a seepage control system.

The seepage control mechanisms are systematically illustrated with examples in nuclear waste disposal, dam engineering and underground engineering, and hence the seepage control effects of each mechanism are demonstrated. A procedure is suggested for performance assessment and optimization design of a seepage control system in geotechnical engineering, which at least has been partly followed and would serve as a cost-effective guidance on control of seepage flow in various engineering practices.

References

[1] Fipps G, Skaggs R W, Nieber J L. Drains as a boundary condition in finite elements. Water Resources Research, 1986, 22 (11): 689–707.

[2] Xu Jiahai. Seepage control of hydraulic structures on sand/gravel foundations. Chinese Journal of Geotechnical Engineering, 1986, 8 (2): 96–106 (in Chinese).

[3] Cao Dunlu, Xu Zhongsheng, Wu Songgui. Seepage control of weakened rock foundation of Gezhouba—Erjiang sluice. Journal of Hydrodynamics (Ser. A), 1987, 2 (2): 25–33 (in Chinese).

[4] Liu Jie, Miao Liangjuan. Safety analysis of the clay core of Zihe soil dam for seepage control. Chinese Journal of Geotechnical Engineering, 1990, 12 (1): 62–72 (in Chinese).

[5] Zhang Ga, Zhang Lianwei, Zhang Jianmin, et al. Seepage analysis for upstream cofferdam of Xiluodu hydropower station. Journal of Hydroelectric Engineering, 2002, (3): 54–61 (in Chinese).

[6] Shen Zhenzhong, Zhang Xin, Lu Xi, et al. Seepage control optimization of left bank of Laohuzui hydropower station. Journal of Hydraulic Engineering, 2006, 37 (10): 1 230–1 234 (in Chinese).

[7] Chen Y F, Lu L S, Zhou C B, et al. Application of the variational inequality approach of Signorini type to an engineering seepage problem. Rock and Soil Mechanics, 2007, 28 (Supp.): 178–182 (in Chinese).

[8] Lu Yumin, Xu Zeping. Methods of seepage analysis of river dikes and seepage control measures. Journal of China Institute of Water Resources and Hydropower Research, 2007, 5 (4): 291–295 (in Chinese).

[9] Chen Y F, Zhou C B, Zheng H. A numerical solution to seepage problems with complex drainage systems. Computers and Geotechnics, 2008, 35 (3): 383–393.

[10] Djehiche A, Kotchev K. Control of seepage in earth dams with a vertical drain. Chinese Journal of Geotechnical Engineering, 2008, 30 (11): 1 657–1 660.

[11] Zhang Nong, Xu Xingliang, Li Guichen. Fissure-evolving laws of surrounding rock mass of roadway and control of seepage disasters. Chinese Journal of Rock Mechanics and Engineering, 2009, 28 (2): 330–335 (in Chinese).

[12] Xie Dingsong, Liu Jie, Wei Yingqi. Key technology problems of seepage control for building high concrete face rockfill dam. Journal of Yangtze River Scientific Research Institute, 2009, 26 (10): 118–121 (in Chinese).

[13] Chen Y F, Hu R, Zhou C B, et al. A new parabolic variational inequality formulation of Signorini's condition for non-steady seepage problems with complex seepage control systems. International Journal for Numerical and Analytical Methods in Geomechanics, 2010, DOI: 10.1002/nag.944 (online published).

[14] Chen Yifeng, Zhou Chuangbing, Mao Xinying, et al. Numerical simulation and assessment of seepage troll effects on surrounding rocks of underground powerhouse in Shuibuya hydropower project. Chinese Journal of Rock Mechanics and Engineering, 2010, 29 (2): 308–318 (in Chinese).

[15] Chen Yifeng, Zhou Chuangbing, Hu Ran, et al. Key issues on seepage flow analysis in large scale hydropower engineering. Chinese Journal of Geotechnical Engineering, 2010 (to be published) (in Chinese).

[16] Yang Qigui, Zhang Jiafa, Xiong Zebin, et al. Seepage field control system for Shuibuya concrete faced rock-fill dam. Journal of Hydroelectric Engineering, 2010, 29 (3): 164–169 (in Chinese).

[17] Chen Y F, Zhou C B, Jing L. Modeling coupled THM processes of geological porous media: theory and validation against laboratory and field scale experiments. Computers and Geotechnics, 2009, 36 (8): 1 308–1 329.

[18] Lai W M, Rubin D, Krempl E. Introduction to continuum mechanics. 3rd ed. Oxford: Pergamon Press Ltd., 1993.

[19] Zhou Y, Rajapakse R K N D, Graham J. A coupled thermoporoelastic

model with thermo-osmosis and thermal-filtration. International Journal of Solids and Structures, 1998, 35(34–35): 4 659–4 683.

[20] Khalili N, Loret B. An elasto-plastic model for non-isothermal analysis of flow and deformation in unsaturated porous media: formulation. International Journal of Solids and Structures, 2001, 38 (46–47): 8 305–8 330.

[21] Zheng H, Liu D F, Lee C F, et al. A new formulation of Signorini's type for seepage problems with free surfaces. International Journal for Numerical Methods in Engineering, 2005, 64 (1): 1–16.

[22] Coussy O. Poromechanics. New York: John Wiley and Sons, Inc., 2004.

[23] Villar M V, Garcia-Sineriz J L, Barcena I, et al. State of the bentonite barrier after five years operation of an in-situ test simulating a high level radioactive waste repository. Engineering Geology, 2005, 80 (3–4): 175–198.

[24] Pusch R. Alteration of the hydraulic conductivity of rock by tunnel excavation. International Journal of Rock Mechanics and Mining Sciences and Geomechanics Abstracts, 1989, 26 (1): 79–83.

[25] Chen Y F, Zhou C B, Sheng Y Q. Formulation of strain-dependent hydraulic conductivity for fractured rock mass. International Journal of Rock Mechanics and Mining Sciences, 2007, 44 (7): 981–996.

[26] Gatabin C. Bentonite THM mock-up experiments, sensors data report TN DPC/SCCME 05-2-A. France: Atomic Energy Company (CEA), 2005.

[27] Chen Yifeng, Zhou Chuangbing, Tong Fuguo, et al. A numerical model for fully coupled THM processes with multiphase flow and code validation. Chinese Journal of Rock Mechanics and Engineering, 2009, 28 (4): 649–665 (in Chinese).

[28] Zhou C B, Chen Y F, Mao X Y, et al. Research report on coupled seepage-flow behaviors of the seepage control system in the Shuibuya hydropower project. Wuhan: Wuhan University, 2009.

[29] Esaki T, Du S, Mitani Y, et al. Development of a shear-flow test apparatus and determination of coupled properties for a single rock joint. International Journal of Rock Mechanics and Mining Sciences, 1999, 36 (5): 641–650.

[30] Chen Y F, Sheng Y Q, Zhou C B. Strain-dependent permeability tensor for coupled M-H analysis of underground opening. In: Proceedings of the 4th Asian Rock Mechanics Symposium. Singapore: World Scientific Publishing, 2006: 271.

[31] Cai F, Ugai K, Wakai A, et al. Effects of horizontal drains on slope stability under rainfall by three-dimensional finite element analysis. Computers and Geotechnics, 1998, 23 (4): 255–275.

[32] Rahardjo H, Hritzuk KJ, Leong EC, et al. Effectiveness of horizontal drains for slope stability. Engineering Geology, 2003, 69 (3–4): 295–308.

[33] Van Genuchten M T. A closed form equation for predicting the hydraulic conductivity of unsaturated soils. Soil Science Society of America Journal, 1980, 44 (5): 892–898.

[34] Vanapalli S K, Fredlund D G. Comparison of different procedures to predict unsaturated soil shear strength. In: Shackelford C D ed. Advances in Unsaturated Geotechnics. New York: ASCE, 2000: 195–209.

[35] Morgenstern N R, Price V E. The analysis of the stability of generalized slip surfaces. Geotechnique, 1965, 15 (1): 79–93.